Journal of Applied Mechanics and Technical Physics, Vol. 42, No. 5, pp. 794–805, 2001

FORMATION AND BASIC PARAMETERS OF VORTEX RINGS

D. G. Akhmetov

UDC 532.5; 532.527

This paper describes an experimental study of the properties of vortex rings with variation of parameters of the air jet expelled from a round nozzle by a special device. Characteristics of the vortex rings were determined by hot-wire anemometer measurements of the velocity field at a certain distance from the nozzle exit where vortex formation is presumably completed. A mathematical model for the formation of a vortex ring based on conservation laws is proposed, and a comparison of theoretical results with experimental data is given.

Extensive studies of the formation and motion of vortex rings over more than hundred years have revealed many regularities in vortex motion of fluids and have provided the basis for recent designs of efficient technological processes, for example, the method of extinguishing powerful fires in spouting gas-oil wells [1–3]. However, adequate theories for describing the formation and structure of vortex rings have not yet been developed. A review of papers devoted to investigation of properties of vortex rings is given in [4]. A complete flow pattern for a real vortex ring was first obtained in [5], where anemometer measurements of the velocity field were performed to obtain geometrical and kinematic characteristics of vortex rings, the streamline structure, and vorticity. Practically identical results were obtained in Sullivan [6]. It is of interest to determine the dependence of characteristics of vortex rings on the parameters determining the conditions of their formation. From this viewpoint, the studies of Maxworthy [7] and Tarasov [8] are most informative. However, in these studies, too, emphasis was on estimation of vortex ring characteristics that are easy to determine experimentally — the radius of a vortex ring and its translational velocity. The characteristics of vortex rings that determine their structure remain to be studied.

Formulation of Experiments. The present paper reports results of experimental investigation of vortex rings formed during pulsed discharge of a submerged jet from a cylindrical nozzle with variation in the parameters determining the formation of a vortex ring. Vortex rings were generated by an experimental setup (Fig. 1a) which consisted of a receiver 1 with compressed air, bypass valve 2, and expansion chamber 3 with an outlet nozzle 4. The shaped channel of the nozzle, which consists of an inlet confuser part and an outlet cylindrical part of length l and outlet radius $R_0 = 0.0375$ m, ensures discharge of the submerged air jet from the chamber with a uniform velocity profile at the nozzle exit. The external surface of the nozzle is conical with cone angle θ. The expansion chamber is connected to the receiver 1 with compressed air through a quick-opening electromagnetic valve 2. When the valve opens, the compressed air passes from the receiver to the chamber and forces the air contained in it to the nozzle. The large swirls and pulsations of air in the chamber produced by the opening of the valve are damped by a system of fine-meshed grids. After a certain time $\tau = 1$–1000 msec, the valve closes and the jet from the nozzle is interrupted. The initial pressure in the receiver was sufficiently large (5 MPa) that it did not change significantly during the discharge time and ensured constant velocity of discharge through the shaped hole of the valve. This ensures constant jet velocity V_0 from the nozzle. The length and volume of the chamber were sufficiently large that the jet ejected from the nozzle was formed from the unperturbed air contained in the chamber before the shot and the gas leaving the receiver was not able to reach the nozzle exit. However, excessive increase in chamber dimensions le to the occurrence of intense low-frequency oscillations in the nozzle, as in a Helmholtz resonator. Small damping holes were drilled on the lateral surface of the chamber to restrict the level of pulsations. The experimental setup ensured identical parameters of the jet and the vortex rings produced by repeated starts. A typical oscillogram of

Lavrent'ev Institute of Hydrodynamics, Siberian Division, Russian Academy of Sciences Novosibirsk 630090.
Translated from Prikladnaya Mekhanika i Tekhnicheskaya Fizika, Vol. 42, No. 5, pp. 70–84, September–October, 2001. Original article submitted May 21, 2001.

0021-8944/01/4205-0794 $25.00

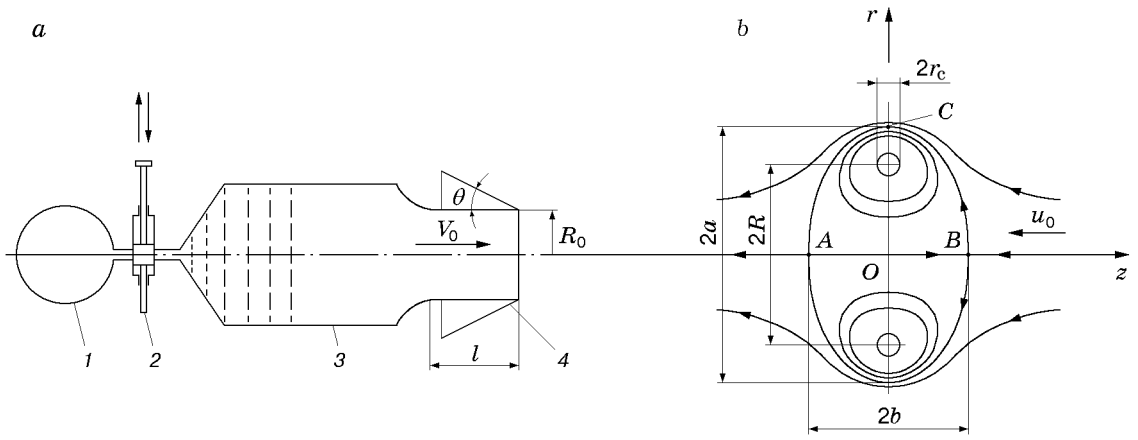

Fig. 1

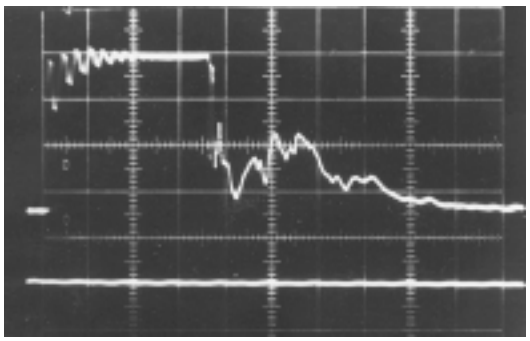

Fig. 2

the hot-wire anemometer signal that characterizes the time variation in jet velocity at the nozzle exit is shown in Fig. 2.

Determining Parameters. From the description of the experimental setup and its operation principle it follows that the formation of a vortex ring during pulsed discharge of a submerged jet from a cylindrical circular nozzle is determined by the following dimensional parameters: the nozzle radius R_0, the length of the cylindrical portion of the nozzle l, the cone angle of the nozzle surface θ, the jet velocity V_0, time of jet discharge τ, and the density and viscosity of the medium ρ and μ, respectively. The current time is not included in the number of determining parameters because the parameters of the vortex ring are determined at the characteristic time — the moment of completion of vortex ring formation, when its further motion can be treated as motion in an unbounded fluid which does not depend on the formation dynamics (this approach to analyzing the motion of turbulent vortex rings was developed in [9]). According to the theory of dimension, from the parameters listed above, one can compose four nondimensional combinations that determine the formation of the vortex ring: $L_* = V\tau/R_0$, $\mathrm{Re} = VR_0\rho/\mu$, θ, and l/R_0.

The experiments were carried out at fixed length of the cylindrical portion of the nozzle $l/R_0 = 2$, the vortex ring parameters were determined with variation of the three nondimensional quantities L_*, Re, and θ, which specify the length of the ejected jet, the Reynolds number of the jet, and the cone angle of the external surface of the nozzle.

To make a similar list of the required parameters of a vortex ring, we can use results of the experimental studies of the vortex ring structure [5] and conclusions from existing theoretical models of vortex rings. According to these data, a vortex ring that has formed can be imagined as a closed volume of swirled liquid with a shape close to an "oblate" ellipsoid of revolution which moves in the surrounding fluid with translational velocity along the minor axis of the ellipsoid. This closed volume of the vortex ring is called the vortex atmosphere. The motion of the medium around the atmosphere of the vortex is similar in pattern to the nonseparation potential flow past the corresponding solid body (see Fig. 1b). Inside the vortex atmosphere, the fluid circulates over closed streamlines

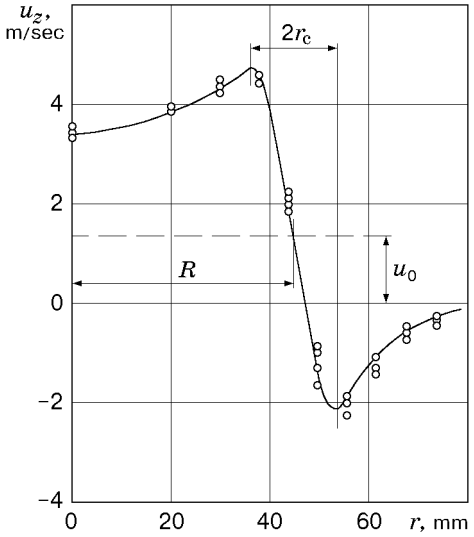

Fig. 3

that enclose the toroidal vortex core. In the meridional section of the vortex, the vorticity distribution has the shape of a bell-shaped curve with maximum at the center of the core, with as much as half of the total vorticity (velocity circulation) concentrated within the core, which, in most cases, occupies only 3–5% of the cross-sectional area of the vortex. Obviously, the main properties of vortex rings with the structure described above are characterized by the following parameters shown in Fig. 1b, where R is the radius of the ring vortex (or the radius of the circular axis of the vortex core), r_c is the radius of the core, a and b are the lengths of the semiaxes of the vortex atmosphere, u_0 is the translational velocity of the ring vortex, Γ is the velocity circulation along the closed streamline $AOBCA$, which envelopes the vortex atmosphere (in Fig. 1, the vortex streamline are presented in a coordinate system attached to the vortex), γ_c is the velocity circulation around the vortex core, v is the volume of the vortex atmosphere, $\boldsymbol{P} = \dfrac{\rho}{2}\displaystyle\int_\tau \boldsymbol{\omega} \times \boldsymbol{r}\, d\tau$ is the vortex momentum of the ring [10], which is proportional to the integral of the vector product of the vorticity $\boldsymbol{\omega}$ and the radius-vector $\boldsymbol{r}$ over the fluid volume.

Using the quantities R_0, V_0, and ρ, we can write the required parameters in nondimensional form: R/R_0, r_c/R_0, u_0/V_0, $\Gamma/(V_0R_0)$, $\gamma_c/(V_0R_0)$, $v/(\pi R_0^3)$, $P/(\rho\pi R_0^3V_0)$, a/R_0, and b/R_0.

Vortex ring parameters were determined from the velocity field measured by hot-wire anemometer probes. The probes were placed at a distance $z = 12R_0$ from the nozzle exit. The distance was chosen such that in all experiments the formation of a vortex ring was completed by the moment when the vortex arrived at to the probes. We used miniature hot-wire probes with a sensor made of a platinum wire of 5 μm diameter and 1 mm length fastened to a thin holder. Assuming axisymmetric flow in the vortex ring and placing the wire of one probe perpendicular to the z and r axes in the axial plane of symmetry of the ring and the wire of the second probe parallel to the z axis, one can obtain the time dependence of the magnitude and direction of the velocity vector in the vortex ring moving through the probes.

At the moment when vortex formation is completed, the motion of the vortex ring is practically steady-state. Therefore, it can be assumed that the vortex structure remains unchanged during passage through the measuring point. Hence, the time dependence of the velocity can be reduced to the dependence of the velocity on the spatial coordinates (z, r) attached to the vortex using the transformation $z = u_0t$, $u = u_1 - u_0$, where t is the current time, u_0 is the translational velocity of the vortex ring (in the z direction), and u_1 and u are the velocity components along the z axis in the laboratory coordinate system and the coordinate system attached to the vortex ring, respectively. Thus, for a fixed position of the probes, it is possible to determine the velocity distributions along the line parallel to the z axis at $r = \text{const}$. The entire flow pattern was determined by discrete displacement of probes on the radial axis r and restart of the vortex, and for each position of the probes, measurements were averaged over four starts of the vortex.

The principle of determining some parameters of the vortex ring is shown in Fig. 3, which gives an exper-

imental plot of the axial velocity component $u_z(0, r)$. The point of intersection of the experimental curve with the straight line $u_z = u_0$ corresponds to the center of the vortex core and determines the vortex radius R. At the vortex core, u_z varies practically linearly. The distance between the extrema at the ends of the linear segment of the curve $u_z(r)$ is equal to the doubled radius of the vortex core $2r_c$. More precisely, the radius of the core is determined from the distributions of the radial velocity component $u_r(z)$ at $r = R_0$ since the largest and smallest peaks on this plot are more pronounced. The lengths of the semiaxes of the vortex ring are determined as follows: as the doubled length of the minor semiaxis $2b$, we use the distance between two points of the distribution $u_z(z, 0)$, where u_z takes zero values (branching point of the streamline on the z axis). To determine the length of the semiaxis a, we calculate the distribution of the stream function $\psi = \int\limits_0 r u_z \, dr$ at $z = 0$. The distance on the r axis between points corresponding to zero values of ψ is equal to a. The velocity circulation around the core $\gamma_c = \oint \boldsymbol{u} \, d\boldsymbol{l} = 2\pi r_c u_c$ is determined from values of the radial velocity u_c on the boundary of the core and the radius of the core.

To determine the translational velocity u_0, we visualized the vortex ring by smoke and illuminated it by a narrow slot-hole light when it moved in the zone of the probes. The lighter was made up of five pulsed lamps, which give five sequential flashes at specified times. Therefore, a frame taken by a photographic camera shows five sequential positions of the vortex. The translational velocity of the vortex ring was determined from measured times of flashes and positions of the vortex on the photograph. In describing experimental results, we use the following nondimensional parameters of the vortex ring (some of them are denoted by asterisk): $R_* = R/R_0$, $\varepsilon = r_c/R$, $u_0^* = u_0/V_0$, $\Gamma_* = \Gamma/(V_0 R_0)$, $\gamma_c^* = \gamma_c/(V_0 R_0)$, $r_c^* = r_c/R_0$, $v_* = v/(\pi R_0^3)$, $P_* = P/(\rho\pi R_0^3 V_0)$, and a/b.

Dependence of Vortex Ring Structure on Jet Length. In the present experiments, vortex rings were produced by discharge of an air jet with fixed velocity $V_0 = 7.3$ m/sec. The radius of the nozzle exit was $R_0 = 37.5$ mm. The Reynolds number of the jet was constant: $\mathrm{Re} = 1.825 \cdot 10^4$. The jet length was varied by changing the time of jet discharge τ. The studies were performed for five values of the jet length: $L = V_0\tau = 70$, 142, 286, 420, and 695 mm. Characteristics of the vortex rings formed for these jet parameters are given in Fig. 4 as functions of the nondimensional jet length $L_* = V_0\tau/R_0$. From Fig. 4 it follows that the main nondimensional parameters of the vortex ring increase rapidly with increase in L_* at $L_* \leqslant 6$–8. With further increase in jet length, the translational velocity u_0^* and ε and γ_c/Γ practically do not change. Only the radii of the vortex R_* and the core r_c^* and the velocity circulation Γ_* continue to increase. In addition, from Fig. 4 it follows that for large values of v_*, the volume of the vortex atmosphere L_* depends linearly on the length of the ejected jet.

Vortex Ring Parameters with Variation in Jet Reynolds Number. The effect of the jet Reynolds number on the vortex ring structure was studied for a constant jet length $L = V_0\tau = 188$ mm ($L_* = 5$). The jet Reynolds number was varied by changing the jet velocity V_0 with corresponding variation in the throat of the quick-acting valve. In order that the jet length $V_0\tau$ remained constant, the time of jet discharge τ was decreased in accordance with increase in the velocity V_0.

Results of flow visualization experiments and results of measurements of vortex ring parameters show follows that two different types of vortex ring formed depending on the jet Reynolds number. For $\mathrm{Re} \leqslant (1$–$2) \cdot 10^4$, laminar vortices with a layered spiral structure formed, which did not change during the further motion of the vortex. The structure of the vortex rings formed for large Re is not layered. The flow in their atmosphere is turbulent. However, visualization of them by smoke shows a well-cut toroidal vortex core. Both types of vortex ring photographed soon after the end of their formation are shown in Fig. 5. Because the vortices were illuminated by a thin flat ray of light, the photographs shows only meridional sections of the vortices. On the right of Fig. 5, the turbulent vortex is shown from the end. It is interesting that along the toroidal core, smoke is distributed in the form of periodical spots, and the core consists of seemingly separate cells bounded by the torus surface and meridional planes. The number of cells in this photograph is 26. Additional studies showed that the cellular smoke structure exists outside the vortex core, and inside of the core is colored uniformly. A comparison of the pattern obtained with the other existing patterns of periodic distribution of fine particles in fluids (for example, aggregation of dust in nodes of standing sound waves in a tube or Taylor vortices between rotational coaxial cylinders) suggests that for particular Re number, near the core there is a secondary axisymmetric flow. Secondary flows of this type can be radial fluid flows directed from the core and to the core at neighboring joints of the cells. Apparently, in this case, the number of cells at the torus should be even. In [7, 11] it is shown that a vortex ring can be unstable against flexural perturbations of the core.

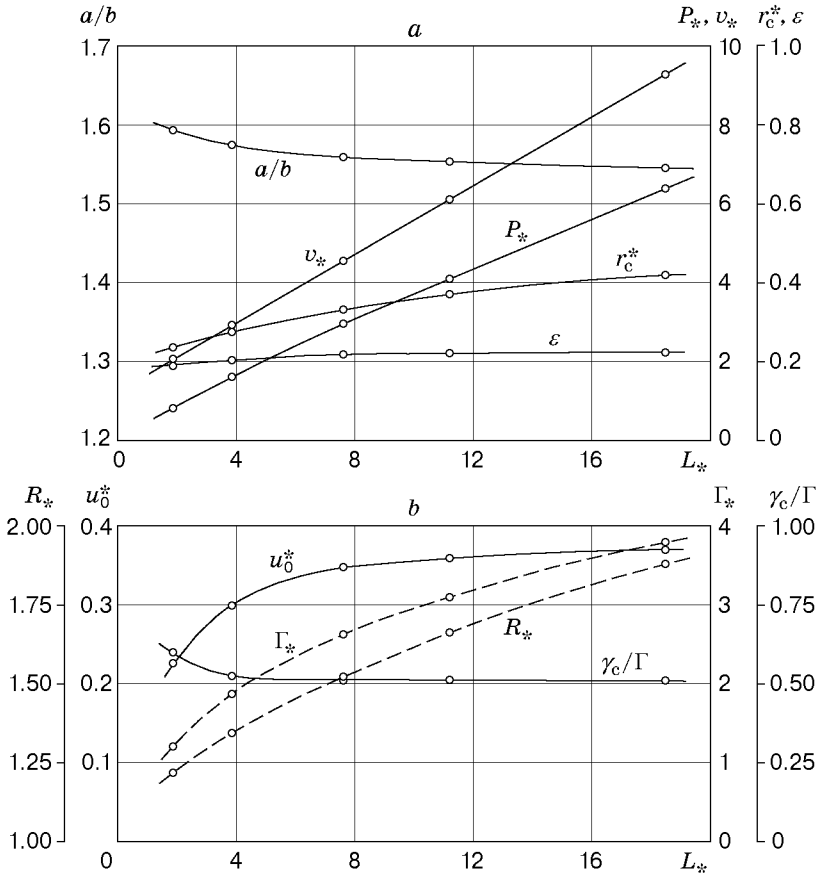

Fig. 4

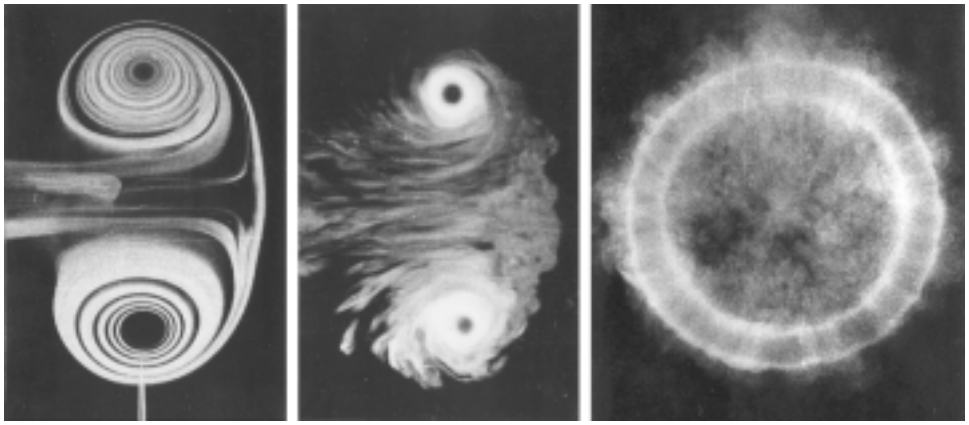

Fig. 5

Results of measurements of vortex ring parameters with variation in Re are given in Fig. 6. From Fig. 6 it follows that the strongest dependence of vortex ring parameters on Re is observed for laminar vortex rings at $\mathrm{Re} \leqslant 10^4$. In this case, the swirled vortex core encompasses a considerable area of the meridional section of the vortex atmosphere, whose shape differs from the spherical shape. Therefore, for small values of Re, the parameter $\varepsilon = r_c/R$ was determined as $\varepsilon \approx \sqrt{s_c/(\pi R^2)}$, where s_c is the cross-sectional area of the swirled vortex core. It is established that the transverse semiaxis of the vortex atmosphere a practically does not depend on Re over the entire range of Re and the longitudinal semiaxis b increases rapidly with decrease in Re. As a result, with decrease in Re, the ratio of the semiaxes a/b tends to unity, i.e., the vortex atmosphere becomes practically spherical. It can be assumed that such vortex rings are similar in structure to a spherical Hill vortex [10]. From Fig. 6a it

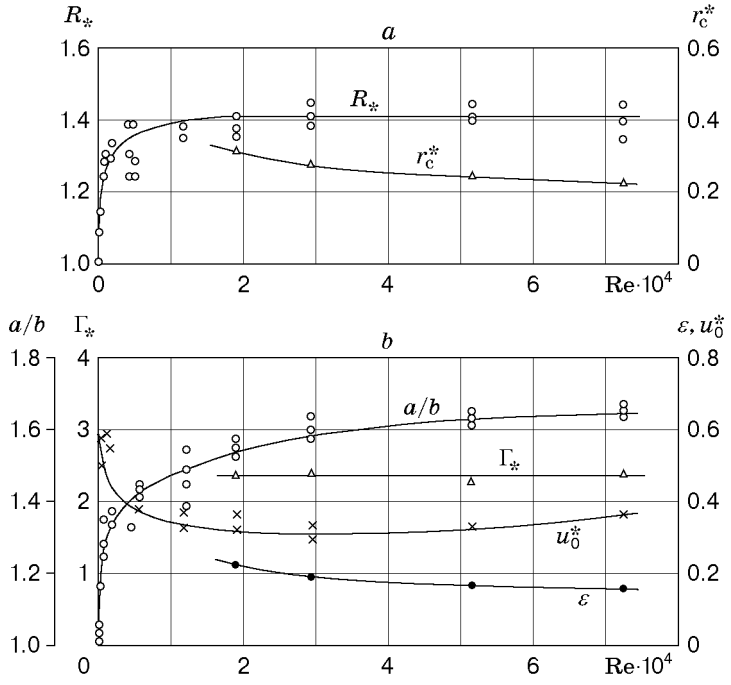

Fig. 6

follows that for Re $\to$ 0, the radius of the vortex ring R_* tends to unity. For very small Re numbers, vortex rings were generated by jet ejection from a 1 cm diameter nozzle by a piston, and the working media were solutions of glycerin in water with large viscosity. In this case, the jet velocity was determined from the piston velocity. In Fig. 6 it can be seen that in transition to the turbulent structure, all vortex ring parameters vary smoothly in a soft mode and not abruptly, as is typical of boundary-layer flows. From Fig. 6 it follows that for Re $>$ (1–2) $\cdot\, 10^4$, the nondimensional radius of the vortex ring R_* and the velocity circulation Γ_* practically does not depend on Re. In this case, the circulation γ_c^* is also nearly constant and has a value of $\gamma_c^* \approx 1.33$. The radius of the core r_c^* decreases with increase in Re, and the translational velocity u_0^* at Re $> 10^4$ varies insignificantly.

Turbulent vortex rings are characterized by considerable angular velocities of the fluid in the core. The mean angular velocity in the core ω_c can be estimated as the ratio of the peripheral velocity u_c on the boundary of the core to the radius of the core. From the data given in Fig. 6 it follows that for Re $= 7.5 \cdot 10^4$, the angular velocity of fluid rotation in the core reaches 35,000 rev/min. In this case, the translational velocity of the vortex ring is about 11 m/sec. In special experiments using a shock tunnel, we obtained vortex rings with a translational velocity of $u_0 \geqslant 100$ m/sec (in particular, $u_0 = 99$ m/sec and $R = 33$ mm for $V_0 = 198$ m/sec and $R_0 = 25$ mm). It can be assumed that in this case, the angular velocity of the fluid in the core is an order of magnitude higher than the above-mentioned value. Indeed, according to measurement results, the mean linear velocity u_c on the boundary of the core for high-velocity vortex rings can be estimated as $u_c \approx (3\text{–}5)u_0$. Because the geometrical dimensions, and, hence, r_c of the vortex ring produced from the shock tunnel, are smaller than those of the vortex described, the above estimates show that in this case, the angular velocity in the core can reach 10^6 rev/min. Of great interest is the distribution of turbulent velocity pulsations in vortex rings because it can be similar in nature to that obtained for other concentrated vortex formations in fluids.

Figure 7 shows oscillograms of hot-wire anemometer signals which record the magnitude of the velocity (upper curve) and the radial velocity component (lower curve) with variation in the z coordinate at $r \approx R_0$, i.e., the velocity was determined along the line that was parallel to the z axis and passed through the vortex core. The oscillograms were obtained for $L_* = 2.5$, Re $= 7.5 \cdot 10^4$, $u_0 = 11$ m/sec, and $R = 51.4$ mm. The minimum values of the signals at the center of the frame correspond to the position of the probes near the center of the vortex core, and the maximum values correspond to the position on the boundary of the core. From the oscillograms it follows (with allowance for the strongly nonlinear dependence of the hot-wire anemometer signal on velocity) that the velocity pulsations on the core boundary reach a large value comparable to the mean value of the velocity in this region. With distance from the core boundary, the pulsations decrease. It should be noted that the velocity pulsations

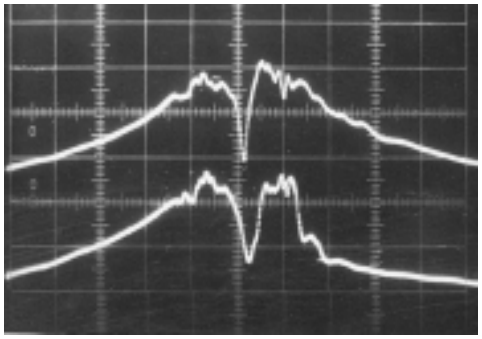

Fig. 7

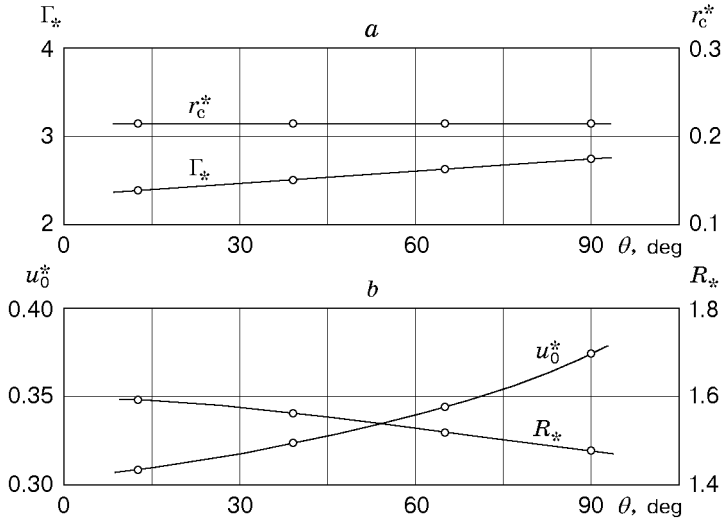

Fig. 8

are not stochastic, unlike the pulsations in the boundary layers, and have some quasiperiodicity. Such structure of the pulsations suggests that they can be caused by deformations (waves) of the core surface, as was observed in studies [12] of vortex cores in flows of various types. In addition, in [12] it is shown that the cross section of vortex cores is not round but has the shape of a polygon, with the number of angles of the polygon changing sporadically in the turbulent regime, and swirled fluid jets are discharged from the angular points of the core into the surrounding medium. With distance from the core, the jets roll themselves up into spiral "sleeves." It is probable that passage of these spiral "sleeves" through the measuring probe determines the nature of the velocity pulsations shown in Fig. 7.

Effect of Nozzle Cone Angle on Vortex Ring Characteristics. In the experiments, we studied vortex ring parameters for $R_0 = 37.5$ mm, $V_0 = 8.1$ m/sec, and $V_0\tau = 230$ mm ($\mathrm{Re} = 2.02 \cdot 10^4$ and $L_* = 6.14$) and the cone angles of the nozzle surface (see Fig. 1): $\theta = 13.13$, 39, 65, and 90°. Sharp-edged nozzles were used in all experiments, and the generator of the nozzle outer cone surface was 200 mm long. Results of this series of experiments are shown in Fig. 8, from which it follows that the vortex ring parameters depend weakly on θ. With increase in θ, the vortex radius R_* decreases only slightly and the translational velocity u_0^* increases.

Estimation of the Most Important Parameters of Vortex Rings Using Conservation Laws. In order to elucidate the physical meaning of the detected experimental regularities and obtain analytical estimates of the main parameters of vortex rings, we consider in more detail the dynamics of formation of a vortex ring. Figure 9 gives camera records of typical phases of vortex ring formation during discharge of a submerged air jet from a circular cylindrical tube. In Fig. 9, the flow patterns were visualized by smoke, the jet flows from the tube from left to right, and the generators of the tubes are denoted by horizontal lines. The asymmetry of the pattern about the axis of the tube on the first frames is caused by the nonuniform initial distribution of the density of the smoke supplied to the tube for flow visualization. Spiral rolling-up of the vortex sheet (vortex formation) begins at

the moment when the front of the jet emerges from the hole (frame 1). As the jet moves, the vortex recedes from the edge of the hole. The leading edge of the mushroom-like head of the vortex is the boundary of the fluid which was in the tube prior to the beginning of jet discharge. From results of experiments it follows that during most of the jet discharge time (except for the initial stage, where $t \ll R_0/V_0$) the velocity of motion of the leading edge of the jet is equal to $V_0/2$, i.e., half the jet velocity. The jet feeding the vortex retains the cylindrical shape when leaving the hole, and only at the entrance to the vortex, its cross section decreases (frame No. 2–5). The core of the vortex ring is formed from the mixing layer of the jet edge, which rolls itself up into a spiral surface at the entrance to the vortex. The surrounding fluid along the jet edge is also entrained in the vortex. The jet discharge ceases between frame Nos. 5 and 6. By this time, the trailing edge of the jet coincides with the exit section of the tube. In what follows, the vortex is filled with the fluid from the jet tail which is between the tube exit and the vortex. It should be noted that the jet tail rolls itself up into a secondary vortex ring, which moves behind the main vortex ring for some time and dissipates soon. In the last frame in Fig. 9, the formation of the vortex ring is practically completed. From the given camera records it follows that practically the entire mass of the ejected jet is entrained in the volume of the vortex ring, and a rather small amount of the surrounding fluid is entrained in the cortex (dark coils of the spiral). This explains the linear increase in the volume v_* of the vortex ring atmosphere with increase in jet length (see Fig. 4a).

For quantitative estimates of vortex ring parameters with variation in jet length, we use the laws of conservation of the vortex momentum and velocity circulation. Figure 10 shows a flow diagram in which a vortex which has traveled distance s from the tube exit is fed by a cylindrical jet of radius R_0 issuing with velocity V_0. Entering the vortex, the jet is compressed, and its boundary, which is a boundary layer separating from the tube edge, rolls itself up into a spiral surface inside the vortex and then transforms into a vortex core. The section where the jet begins to narrow is at distance λ from the tube exit. Thus, at the distance λ, the jet is weakly perturbed, and only at $z > \lambda$, the effect of the velocity field induced by the vortex itself becomes significant. It can be assumed that the part of the jet to the right of the section $z = \lambda$ has already entered the vortex. Let us estimate the change of vortex momentum in the fluid outside the tube due to jet discharge. It is known that the vortex momentum $\boldsymbol{P}$ is determined by the integral over the fluid volume [10, 13] $\boldsymbol{P} = \dfrac{\rho}{2}\displaystyle\int_\tau \boldsymbol{\omega} \times \boldsymbol{r}\, d\tau$, where ρ is the density of the medium, τ is the fixed volume of integration, which corresponds to the space filled with the fluid outside the tube. The time variation of vortex momentum is given by the equation $\dfrac{\partial \boldsymbol{P}}{\partial t} = \dfrac{\rho}{2}\displaystyle\int_\tau \boldsymbol{r} \times \frac{\partial \boldsymbol{\omega}}{\partial t}\, d\tau$, which by virtue of the equality $\partial\boldsymbol{\omega}/\partial t = \operatorname{rot}(\boldsymbol{u} \times \boldsymbol{\omega})$, where $\boldsymbol{u}$ is the velocity vector, reduces to integrals over the fixed surface Σ bounding the fluid outside the tube:

$$\frac{\partial \boldsymbol{P}}{\partial t} = \frac{\rho}{2}\iint_\Sigma \Big\{\boldsymbol{n}[\boldsymbol{r} \cdot (\boldsymbol{u} \times \boldsymbol{\omega})] - (\boldsymbol{n} \cdot \boldsymbol{r})(\boldsymbol{u} \times \boldsymbol{\omega}) + \boldsymbol{n}q^2 - 2(\boldsymbol{n}\boldsymbol{u})\boldsymbol{u}\Big\}\, d\Sigma.$$

Here $\boldsymbol{n}$ is the outer normal to $d\Sigma$ and $q = |\boldsymbol{u}|$. In the of estimation of $\partial\boldsymbol{P}/\partial t$, integration near the tube exit is performed over the outer surface of the tube, where $\boldsymbol{u} = \boldsymbol{\omega} = 0$, and over the tube exit section. In the tube exit flow, two typical zones are distinguished: the zone of boundary layer flow of thickness δ along the tube wall and the zone of jet flow itself with $\boldsymbol{u} = \boldsymbol{V}_0$ and $\boldsymbol{\omega} = 0$. On the inner surface of the boundary layer the velocity is equal to the jet velocity $\boldsymbol{V}_0$, and on the outer surface of the tube, which coincides with the inner surface of the tube, $\boldsymbol{u} = 0$. Therefore, considering the small thickness of the boundary layer, over the entire cross section of the boundary layer, on the average, we can set $\boldsymbol{u} = (V_0/2)\boldsymbol{k}$ and $\boldsymbol{\omega} = (V_0/\delta)\boldsymbol{e}$, where $\boldsymbol{k}$ is the unit vector in the z direction and $\boldsymbol{e}$ is the unit vector directed counterclockwise along the azimuthal coordinate if one looks at the tube exit from outside. In the integration, it was assumed that $\delta/R_0 \ll 1$ and terms of the order of δ/R_0 and higher were rejected as negligibly small. The calculations show that the vector $\partial\boldsymbol{P}/\partial t$ is directed along the z axis and $\partial P_z/\partial t = \rho\pi R_0^2 V_0^2$. Hence, the total change in the fluid vortex momentum of the fluid over the jet discharge time τ is

$$P_z = \int_0^\tau \frac{\partial P_z}{\partial t}\, dt = \rho\pi R_0^2 V_0^2 \tau.$$

Obviously, at the time $t = \tau$, P_z is the sum of the momentum P of the vortex ring and the momentum of the tail of the vortex layer $P_\lambda = \rho\pi R_0^3 \lambda V_0$. However, as follows from Fig. 9, the evolution of the vortex ring continues even after the cessation of jet discharge. The tail of the vortex sheet becomes a small vortex ring, which

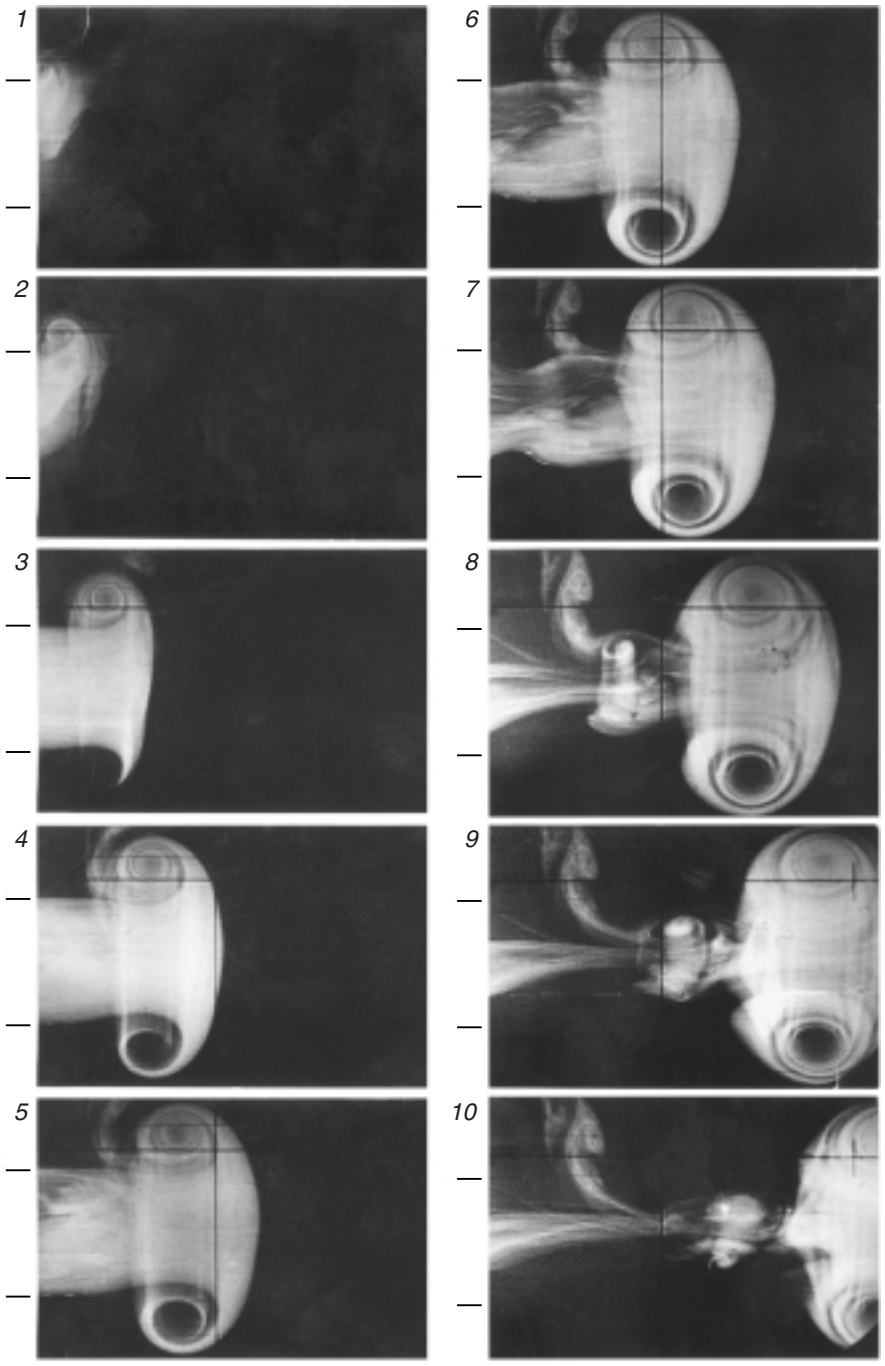

Fig. 9

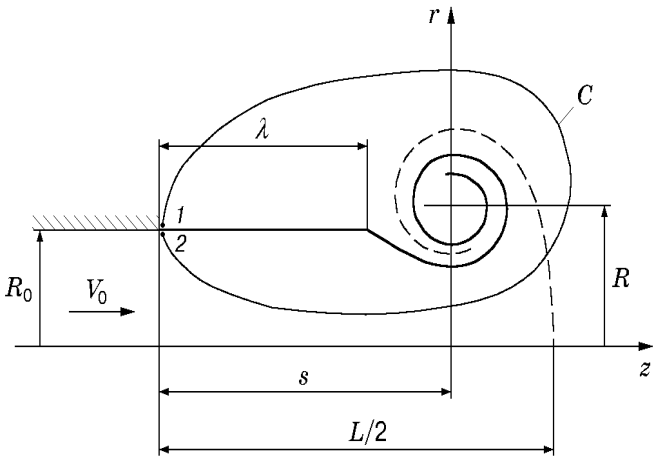

Fig. 10

closes the trailing edge of the jet. This vortex formation with momentum δP is no longer part of the main vortex ring and dissipates soon. It can be assumed that the quantity δP is proportional to P_λ, i.e., $\delta P = \alpha P_\lambda$, where α is a proportionality factor of the order of unity. Therefore, for the moment of completion of vortex ring formation, the momentum of the vortex ring can be written as

$$P = P_z - \delta P. \tag{1}$$

It is known that for $\varepsilon \ll 1$ [10, 14], the momentum P is expressed in terms of the radius R and the circulation Γ of the vortex ring by the formula $P \approx \pi\rho R^2\Gamma$. Therefore, from (1) it follows that

$$\pi\rho R^2\Gamma = \pi\rho R_0^2 V_0^2 \tau - \alpha\pi\rho R_0^3 \lambda V_0. \tag{2}$$

To determine the dependences of R_* and Γ_* on L_* by formula (2), we consider the law of conservation of circulation. It should be noted that during a short initial period $t_0 \ll R_0/V_0$, the jet velocity near the nozzle exit section cannot be considered constant because at $t = 0$, the intensity γ of the vortex layer on the nozzle wall can be written as $\gamma = A/\sqrt{z}$ [15, 16], where z is the distance from the exit edge into the depth of the tubes. At this stage, the flow near the tube edge is assumed to be self-similar and determined only by the coefficient A. The self-similar stage of rolling-up of a vortex sheet shedding from a tube was studied in [15, 17], but in estimations of vortex ring parameters for large times of jet discharge $\tau \gg t_0$, this initial flow stage is not significant. Therefore, it is assumed that during the entire time of jet discharge from the nozzle, the jet velocity is equal to V_0, and the effect of the self-similar stage of the process can be allowed for by assuming that even by the initial time $t = 0$, the velocity circulation in the fluid has value Δ, and the further increase in velocity circulation Γ_C over the contour C in the fluid proceeds at constant velocity V_0 of jet discharge. One might expect that for large values of τ, the quantity Δ is small in comparison with Γ_C. It should be noted that during formation of the vortex ring, the single swirled region in the fluid is the jet boundary surface formed from the boundary layer issuing from the nozzle (see Fig. 10). Considering this surface thin when estimating Γ_C, we draw a cut on it. Then, over the entire space, the flow can be considered irrotational with unique velocity potential φ. To estimate Γ_C, we draw an immovable contour C which envelopes the spiral end of the cut and has ends at points 1 and 2 on different sides of the cut on the hole edge. We calculate the velocity circulation over this contour with allowance for its initial value Δ:

$$\Gamma_C = \Delta + \oint\limits_C u\,dl = \Delta + \oint\limits_C \frac{\partial\varphi}{\partial l}\,dl = \Delta + \varphi_1 - \varphi_2.$$

The potential difference can be estimated from the Cauchy integral of the equations of motion of an ideal fluid written for points 1 and 2:

$$\frac{\partial\varphi_1}{\partial t} + \frac{V_1^2}{2} + \frac{p_1}{\rho} = \frac{\partial\varphi_2}{\partial t} + \frac{V_2^2}{2} + \frac{p_2}{\rho}.$$

Because at points 1 and 2, the pressure is the same: $p_1 = p_2$ (which is indicated, in particular, by the linearity of the jet edge at the nozzle exit), $V_1 = 0$, $V_2 = V_0$,

$$\Gamma_C = \Delta + \varphi_1 - \varphi_2 = \Delta + \frac{1}{2}\int_0^\tau (V_2^2 - V_1^2)\,dt = \Delta + \frac{V_0^2\tau}{2}.$$

Because $\tau = L/V_0$, $\Gamma_C = \Delta + V_0 L/2$ is the total circulation in the fluid at the moment of termination of jet discharge $t = \tau$. At this time, the fluid contains only two vortex formations — the vortex ring with circulation Γ and the tail of the vortex sheet of length λ with circulation $\Gamma_\lambda = \lambda V_0$ (see Fig. 10). Hence, at $t = \tau$, $\Gamma_C = \Gamma + \Gamma_\lambda$. We can assume that in the vortex ring, the velocity circulation Γ does not change even after cessation of jet discharge, because at $t > \tau$, a vortex closing the jet is formed from the tail of the vortex sheet. This vortex remains outside the vortex ring and dissipates (see Fig. 9). Therefore, the velocity circulation of the vortex ring formed can be written as

$$\Gamma = \Delta + V_0(L/2 - \lambda). \tag{3}$$

As was noted above, the rate of propagation of the leading edge of the jet is equal to $V_0/2$. Therefore, the quantity $L/2 - \lambda$ is the distance between the leading edge of the jet and the jet tail at $t = \tau$. On this interval, the spirally rolled head of the vortex sheet is located. From Figs. 9 and 10, it is evident that the transverse dimensions of the spiral formation inside the vortex ring and the segment $L/2 - \lambda$ are comparable in magnitude. Therefore, it can be assumed that the quantity $L/2 - \lambda$ is proportional to the doubled radius of the external coil of the spiral part of the vortex sheet, which is approximately equal to the difference of the radii of the vortex ring and the tube. This is proved by experimental data, from which it follows that

$$L/2 - \lambda \approx 2(R - R_0)K, \tag{4}$$

where K is the proportionality factor.

Writing expressions (2)–(4) obtained from the laws of conservation of the vortex momentum and circulation and from elementary geometrical considerations, we arrive at the following system of equations for R_*, Γ_*, and $\lambda_* = \lambda/R_0$ in nondimensional form:

$$R_*^2\Gamma_* = L_* - \alpha\lambda_*, \quad \Gamma_* = \Delta_* + L_*/2 - \lambda_*, \quad L_*/2 - \lambda_* = 2K(R_* - 1).$$

Here $\Delta_* = \Delta/R_0$. These formulas correspond to experimental data in the examined range of L_* for the following values of empirical constants: $\Delta_* = 0.385$, $\alpha = 0.91$, and $K \approx 2$. The system obtained reduces (by elimination of the quantity λ_*, which is of no interest) to two cubic equations for the radius $R_*(L_*)$ and circulation $\Gamma_*(L_*)$ of the vortex ring

$$\begin{gathered} R_*^3 - [1 - \Delta_*/(2K)]R_*^2 - \alpha R_* - [(1 - \alpha/2)/(2K)L_* - \alpha] = 0, \\ \Gamma_*^3 - 2(2K - \Delta_*)\Gamma_*^2 + [(2K - \Delta_*)^2 - 4\alpha K^2]\Gamma_* - 4K^2[(1 - \alpha/2)L_* - \alpha\Delta_*] = 0. \end{gathered} \tag{5}$$

From results of numerical solutions of these equations (dashed curves in Fig. 4b) it follows that the obtained analytical dependences of R_* and Γ_* on L_* agree with experimental data over the entire range of L_*.

Unfortunately, we were unable to obtain a formula for estimating another important parameter of vortex rings — translational velocity u_0. The translational velocity of a vortex ring with a thin core ($\varepsilon \ll 1$) is known to be given by $u_0 = f\Gamma/(2\pi R)$, where f depends on ε and the distribution law Γ in the vortex core [11, 14]. Such dependence of u_0 on Γ and R follows, generally speaking, from considerations of dimensions. Apparently, to estimate ε and the type of the function f, one needs to solve a more complicated problem of the rolling-up of a vortex sheet with allowance for the viscosity of the medium. Attempts to estimate u_0 using the energy conservation law and additional assumptions on the distribution of Γ in the vortex ring core (proposed, for example, in [18]) seems to be unjustified because of difficulties in taking into account energy dissipation during breakup of the jet tail. However, it should be noted that in the range of L_* considered in the present paper, the values of the function f are in a narrow interval (1.5–1.2), and this makes it possible to estimate (even if roughly) the translational velocity of the vortex ring u_0 using the values of R_* and Γ_* obtained from (5).

The author thanks V. K. Sheremetov for assistance in the experiments and also T. D. Akhmetov and B. A. Lugovtsov for useful discussions of the work.

REFERENCES

1. D. G. Akhmetov, B. A. Lugovtsov, and V. F. Tarasov, "Extinguishing gas and oil well fires by means of vortex rings," *Fiz. Goreniya Vzryva*, No. 5, 8–14 (1980).
2. D. G. Akhmetov and V. F. Tarasov, "Extinguishing fire of a powerful gas fountain," in: *Dynamics of Continuous Media* (collected scientific papers) [in Russian], No. 62, Novosibirsk (1983), pp. 3–10.
3. D. G. Akhmetov, B. A. Lugovtsov, and V. A. Maletin, "Vortex powder method for extinguishing fire on spouting gas-oil wells," in: *Prevention of Hazardous Fires and Explosions*, Kluwer Acad. Publ., Dordrecht, etc. (1999), pp. 319–328.
4. K. Shariff and A. Leonard, "Vortex rings," *Annu. Rev. Fluid Mech.*, **24**, 235–279 (1992).
5. D. G. Akhmetov and O. P. Kisarov, "Hydrodynamic structure of a vortex ring," *Prikl. Mekh. Tekh. Fiz.*, No. 4, 120–123 (1966).
6. J. P. Sullivan, S. E. Widnall, and S. Ezekiel, "Study of vortex rings using a laser doppler velocimeter," *AIAA J.*, **11**, 384–1389 (1973).
7. T. Maxworthy, "Some experimental studies of vortex rings," *J. Fluid Mech.*, **81**, 465–495 (1977).
8. V. F. Tarasov, "Estimation of some parameters of a turbulent vortex ring," in: *Dynamics of Continuous Media* (collected scientific papers) [in Russian], No. 14, Novosibirsk (1973), pp. 120–127.
9. B. A. Lugovtsov, "Turbulent vortex rings," in: *Dynamics of Continuous Media* (collected scientific papers) [in Russian], No. 38, Novosibirsk (1979), pp. 71–88.
10. H. Lamb, *Hydrodynamics*, Cambridge Univ. Press (1932).
11. S. E. Widnall, D. B. Bliss, and C.-Y. Tsai, "The instability of short waves on a vortex ring," *J. Fluid Mech.*, **66**, 35–47 (1974).
12. D. G. Akhmetov and V. F. Tarasov, "On the structure and evolution of vortex cores," *Prikl. Mekh. Tekh. Fiz.*, **5**, 68–73 (1986).
13. G. K. Batchelor, *Introduction to Fluid Dynamics*, Cambridge Univ. Press, Cambridge (1967).
14. L. E. Fraenkel, "Examples of steady vortex rings of small cross-section in an ideal fluid," *J. Fluid Mech.*, **51**, 119–135 (1972).
15. D. I. Pullin, "Vortex ring formation at tube and orifice openings," *Phys. Fluids*, **22**, 401–403 (1979).
16. G. Bardotti and B. Bertotti, "Magnetic configuration of a cylinder with infinite conductivity," *J. Math. Phys.*, **5**, 1387–1390 (1964).
17. P. G. Saffman, "The member of waves on unstable vortex rings," *J. Fluid Mech.*, **84**, 625–639 (1978).
18. V. A. Vladimirov and V. F. Tarasov, "Formation of vortex rings," *Izv. Sib. Otdel. Akad. Nauk SSSR, Ser. Tekh. Nauk*, No. 3, Issue 1, 3–11 (1980).